journal of the mechanical behavior of biomedical materials 152 (2024) 106434

Contents lists available at ScienceDirect

Journal of the Mechanical Behavior of Biomedical Materials

journal homepage: www.elsevier.com/locate/jmbbm

Quantification of long-term nonlinear stress relaxation of bovine trabecular bone

Thomas Gersie [a,*], Thom Bitter [a], David Wolfson [b], Robert Freeman [b], Nico Verdonschot [a,c], Dennis Janssen [a]

[a] Radboudumc, Orthopaedic Research Lab, PO Box 9101, 6500 HB, Nijmegen, Netherlands
[b] DePuy Synthes Joint Reconstruction, WW Research & Development, LS11 OBG, Leeds, UK
[c] University of Twente, Faculty of Science and Technology, 7522LW, Enschede, Netherlands

ARTICLE INFO

Keywords:
Stress relaxation
Time-dependent
Nonlinear viscoelasticity
Trabecular bone
Bone mineral density
Schapery model
Superposition model

ABSTRACT

The reliability of computational models in orthopedic biomechanics depends often on the accuracy of the bone material properties. It is widely recognized that the mechanical response of trabecular bone is time-dependent, yet it is often ignored for the sake of simplicity. Previous investigations into the viscoelastic properties of trabecular bone have not explored the relationship between nonlinear stress relaxation and bone mineral density. The inclusion of this behavior could enhance the accuracy of simulations of orthopedic interventions, such as of primary fixation of implants. Although methods to quantify the viscoelastic behavior are known, the time period during which the viscoelastic properties should be investigated to obtain reliable predictions is currently unclear. Therefore, this study aimed to: 1) Investigate the duration of stress relaxation in bovine trabecular bone; 2) construct a material model that describes the nonlinear viscoelastic behavior of uniaxial stress relaxation experiments on trabecular bone; and 3) implement bone density into this model. Uniaxial compressive stress relaxation experiments were performed with cylindrical bovine femoral trabecular bone samples (n = 16) with constant strain held for 24 h. Additionally, multiple stress relaxation experiments with four ascending strain levels with a holding time of 30 min, based on the results of the 24-h experiment, were executed on 18 bovine bone cores. The bone specimens used in this study had a mean diameter of 12.80 mm and a mean height of 28.70 mm. A Schapery and a Superposition model were used to capture the nonlinear stress relaxation behavior in terms of applied strain level and bone mineral density. While most stress relaxation happened in the first 10 min (up to 53 %) after initial compression, the stress relaxation continued even after 24 h. Up to 69 % of stress relaxation was observed at 24 h. Extrapolating the results of 30 min of experimental data to 24 h provided a good fit for accuracy with much improved experimental efficiency. The Schapery and Superposition model were both capable of fitting the repeated stress relaxation in a sample-by-sample approach. However, since bone mineral density did not influence the time-dependent behavior, only the Superposition model could be used for a group-based model fit. Although the sample-by-sample approach was more accurate for an individual specimen, the group based approach is considered a useful model for general application.

1. Introduction

The reliability of computational models of bone biomechanics in orthopedic applications, such as total joint reconstructions or bone fracture repair, depends on the accuracy of the bone material properties. Trabecular bone is generally modelled as a linear time-independent elastic material in which the Young's modulus is related to the density of the bone (Pankaj, 2013; Taylor et al., 2012; van der Ploeg et al., 2012). Although it is widely recognized that the mechanical response of trabecular bone is time-dependent, it is often ignored for the sake of simplicity (Schoenfeld et al., 1974; Zilch et al., 1978). However, in some cases, such as in the analysis of primary stability of press-fit implants, the viscoelastic behavior may have a significant effect on the biomechanics.

The viscoelastic response of trabecular bone has been experimentally investigated either using relaxation tests in which the time-dependent

* Corresponding author.
E-mail address: Thomas.gersie@radboudumc.nl (T. Gersie).

https://doi.org/10.1016/j.jmbbm.2024.106434
Received 9 June 2023; Received in revised form 11 January 2024; Accepted 25 January 2024
Available online 3 February 2024

change in stress under an applied constant strain is measured over time (Schoenfeld et al., 1974; Zilch et al., 1978; Deligianni et al., 1994; Bredbenner et al., 2006; Quaglini et al., 2009), or in creep tests in which the change in strain under an applied constant load is measured over time (Bowman et al., 1994; Manda et al., 2016, 2017; Yamamoto et al., 2006). It has previously been shown that the linear time-dependent relaxation modulus is correlated to the density of bone, thus playing a prominent role in predicting viscoelasticity (Manda et al., 2016). However, the magnitude of the time-dependent response is affected by the applied stress/strain level (Quaglini et al., 2009; Yamamoto et al., 2006; Bowman et al., 1998), making it incorrect to be modelled using linear viscoelasticity. Hence, a nonlinear viscoelastic material model that takes bone density into account should be constructed.

The time period during which the viscoelastic properties are being investigated are important to obtain a reliable indication of the extent of stress relaxation or creep. In previous research the holding time of the constant strain/stress was as short as 100 s, while others showed a decreasing stress even after 1000 s (Schoenfeld et al., 1974; Burgers et al., 2009). Thus, there is no consensus of the required experimental time based on current literature, while the duration of the stress relaxation behavior of bone may be of significant importance. Accordingly, the effect of duration on stress relaxation should be investigated.

From the above, it is clear that the relationship between bone density and the nonlinear stress relaxation of the trabecular bone at different strain levels should be quantified. Therefore, the objectives of this study were to: 1) Investigate the duration of stress relaxation in bovine trabecular bone; 2) construct a material model that describes the nonlinear viscoelastic behavior of uniaxial stress relaxation experiments on bovine trabecular bone; and 3) implement the bone density into this model.

2. Materials and methods

To accomplish the three aforementioned objectives, two separate experiments were conducted. Firstly, a 24-h stress relaxation experimented was performed to examine the duration of stress relaxation in trabecular bone. Secondly, repeated stress relaxation experiments were used to establish a viscoelastic material model that incorporates the dependence on BMD. Subsequently, the fit accuracy and experimental testing time was optimized using the 24-h experimental data. Additionally, the two nonlinear models were fitted on the data of the repeated stress relaxation experiments.

2.1. Sample preparation

Six distal bovine femora (male, age under 30 months) were obtained from a local abattoir and stored individually at −16 °C in plastic bags prior to usage. Most of the cortical bone was removed using an oscillating saw (Conmed, USA), whereafter cylindrical bone cores were extracted from the trochlear region and from the anterior and posterior condyles using a diamond core drill bit (Articomed, Poland) (Fig. 1). The drill bit had an inner diameter of 12.85 mm and a length of 70 mm. A low-speed rotating saw (Conmed, USA) was used to create parallel sections and to remove remaining cortical bone at the articulating surface, thereby creating a cylindrical sample only consisting of trabecular bone. Coring and cutting was performed on frozen femurs in air. In total 34 samples were harvested with a diameter of 12.80 ± 0.05 mm and a mean height of 28.70 ± 0.70 mm, which were of similar size as in previous studies (Quaglini et al., 2009; Manda et al., 2016). Bone cylinders were wrapped in saline-soaked gauze and stored in separate plastic airtight containers at −16 °C. Before testing each end of the thawed cylindrical sample was fixed using bone cement (polymethyl-methacrylate, Candulor, Switzerland) in aluminum endcaps to minimize end-artefacts during compression testing (Keaveny et al., 1997). To determine the average strain for each specific bone sample, the effective length (25.50 ± 0.56 mm) was calculated as the length of the sample between the endcaps plus half the length of the sample embedded within the endcaps (Keaveny et al., 1997). A height-to-width ratio of 2.0 was chosen to avoid buckling of the samples during compression (Zhao et al., 2018). An example of a bone specimen embedded in the endcaps can be seen in Fig. 2.

2.2. CT imaging

Before extraction of the bone samples, computed tomography (CT) images were made of each drilled distal femur with a voxel size of 0.5 × 0.47 × 0.47 mm (Canon medical systems, Japan – 80 kV 250 mA) along with a solid calibration phantom (Image Analysis, USA) (Eggermont et al., 2019). In-house developed software was used to convert Hounsfield Units to calibrated BMD values (Derikx et al., 2011). A cylindrical model was aligned with the (drilled) specimen in the CT scan after which an average BMD was calculated for each specimen. All cylinders were then sorted based on their average BMD value.

2.3. Stress relaxation experiments

After being embedded in the endcaps, the samples were placed in the testing environment, which consisted of a water basin filled with

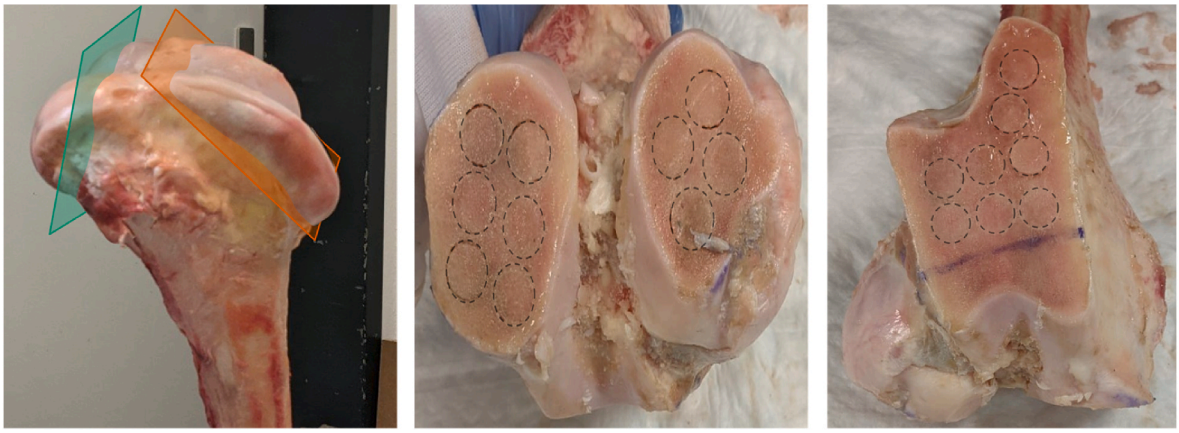

Fig. 1. Overview of coring and cutting locations. On the left picture, the cutting planes on the distal femur are shown. The green plane shows the cut through the cortex of the condyles and the orange plane shows the trochlear cut. In the middle image, the drilling holes and thereby specimen locations in the condyles are shown. On the right, the specimens locations in the trochlea of this particular bovine femur are displayed.

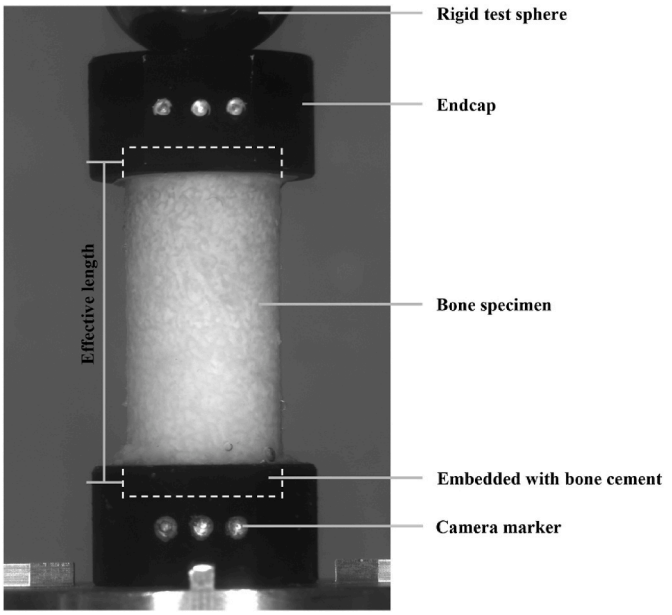

Fig. 2. Picture of a bone specimen embedded in endcaps with bone cement made by the camera system to measure actual displacement of the bone specimen using the camera markers on the endcaps. The effective length is defined as the length of the sample between the endcaps plus half the length of the sample embedded within the endcaps. On top of the upper endcap, a rigid test sphere was placed to accommodate for slight angular variations of the sample and endcap.

physiological saline, supplemented with 1 % penicillin/streptomycin (Capricorn scientific, Germany), with a temperature of 37.0 ± 0.5 °C. After 30 min in the basin, each sample was preconditioned by applying ten cycles of 0.1 % strain and was allowed to recover for 30 min, which is similar to previous studies (Bowman et al., 1994). Stress relaxation experiments were conducted using an MTS machine (MTS Systems Corporation, USA) with a measuring frequency of 10 Hz (24-h of stress relaxation) and 100 Hz (repeated stress relaxation experiments). The sample was compressed using a rigid test sphere on top of the upper endcap (Fig. 2). Static strains of 0.2, 0.4, 0.6, and 0.8 % were applied to measure the viscoelastic response to stay below the yield strain of 0.8 % of bovine trabecular bone (Kopperdahl et al., 1998). The strains were applied and removed at a strain rate of 0.01 s^{-1}. A 500 N loadcell (type AT101 – 0.5/5) was used when applying 0.2 % strain. At higher strain levels, a 15 kN (type 2816) loadcell was used. An overview of the stress relaxation experiments is displayed in Fig. 3.

A digital camera (Pixelink, Canada) was used to optically measure the axial displacement applied to the bone samples. Markers on the endcaps (Fig. 2) were used to calculate the actual strains the samples were subjected to. Images were calibrated using a reference object in the field of view. Prior testing showed the accuracy of our system to be 2 μm. Images of the uniaxial compression test were continuously captured (2 images/second for the first 30 s, then 1 image each 30 s) and deformations of the samples were calculated using a custom-written Matlab script (Matlab R2021b, USA).

2.3.1. *Twenty-four hours stress relaxation*

To determine if the strain level influenced the duration of stress relaxation of trabecular bone, four specimens per strain level were selected to ensure homogeneous distribution of the BMD. Therefore, 16 samples were used in total. Each sample was subjected to a single static strain level for 24 h to measure the duration of the stress relaxation response.

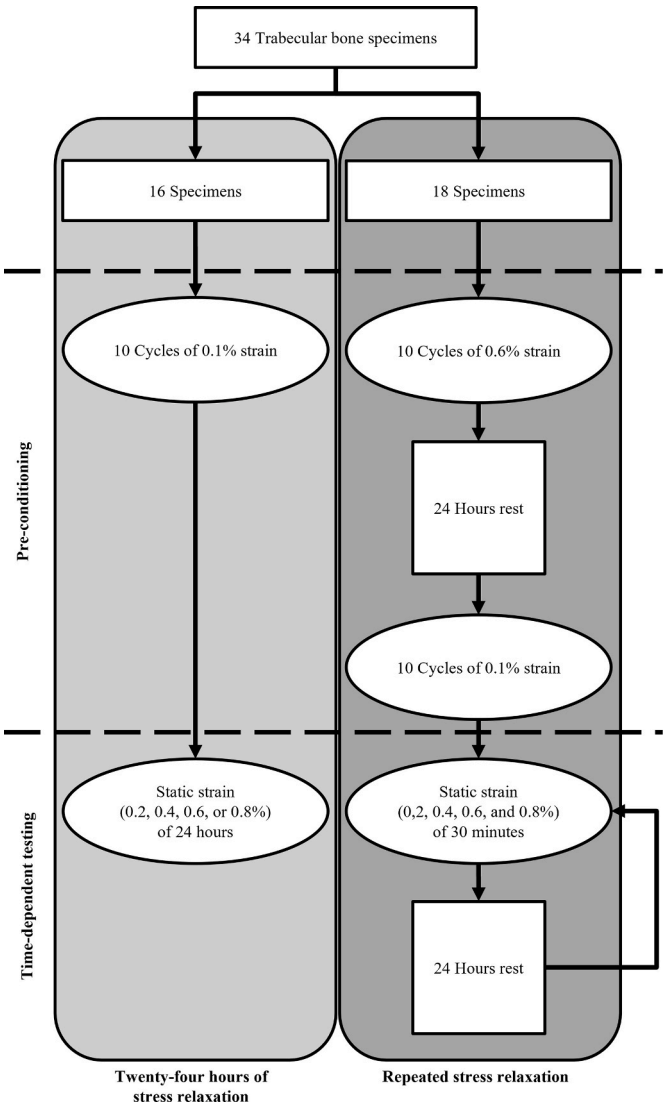

Fig. 3. Overview of executed stress relaxation experiments.

2.3.2. *Repeated stress relaxation*

The remaining 18 samples were used for the repeated stress relaxation and were pre-conditioned at 0.6 % strain for ten cycles and were then allowed to recover for 24 h. This strain level was chosen because no plastic deformation was observed during the 24 h stress relaxation. By increasing the strain level, our goal was to enhance repeatability, which is even more important in the repeated stress relaxation experiments. Repeated stress relaxation experiments were conducted on the samples to examine the influence of applied strain level on the time-dependent response, without interference of the specific properties of that individual sample. These samples were compressed on four consecutive days at increasing static strains from 0.2 to 0.8 %, with 0.2 % increments. Prior to the static strain, the samples were subjected to ten cycles of 0.1 % strain as described previously and were allowed to recover for 30 min. After each experiment the sample was allowed to recover in saline at 5 °C for 24 h, as it has been demonstrated that bone fully recovers within this timeframe (Deligianni et al., 1994). The holding time of the constant strain was determined after analysis of the 24-h experiments with the aim to determine a feasible testing time which included most of the stress relaxation behavior.

2.4. Experimental testing time

To optimize fit accuracy and experimental testing time, the data of the 24-h experiment were analyzed in the following manner. First, the stress relaxation modulus was calculated using the actual strain data, obtained by the camera. Thereafter, the first 10, 30, 60, and 120 min of data per experiment were used to create a power law representation (eq (1).) of the relaxation modulus (E(t)). Using the power law representation each data set was extrapolated to 24 h.

$$E(t) = E_1 + E_2 t^n \tag{1}$$

where E_1, E_2 and n are constants. Fitting was carried out in Matlab using the curve fitting toolbox, by minimizing the error using nonlinear least squares (Matlab R2021b, Mathworks, USA). The mean percentual error was calculated to determine which experimental time showed the optimal trade-off between fit accuracy and testing time. This experimental time was then used as the holding time of the constant strain as explained in 2.3.2.

2.5. Nonlinear viscoelastic models

To capture the effect of applied strain level on the time-dependent mechanical properties, two nonlinear viscoelastic models were considered in this study. In previous studies, these models were successful in describing nonlinear stress relaxation in dentin and ligaments (Emamian et al., 2021; Provenzano et al., 2002). The material models were fitted to the repeated stress relaxation experiments after extrapolation to 24 h. It was assumed that the strain rate of 0.01 s^{-1} was sufficiently fast to act as instantaneous for the strains examined in this study. As a result, the initial ramp to the maximum force before the stress relaxation was considered as a step and excluded from the fitting process (Manda et al., 2017). Fitting was carried out using the same procedure as described previously in section 2.4.

2.5.1. Simplified Schapery method (SSM)

The original Schapery model was simplified by considering a given strain, ε_0, as a step function, setting h_1 and α_ε to unity, and where the transient modulus is in the form of a power law ($C^* t^n$) (Provenzano et al., 2002; Schapery, 1969):

$$\sigma(\varepsilon_0, t) = h_e(\varepsilon_0) E_e \varepsilon_0 + h_2 \varepsilon_0 C t^n \tag{2}$$

in which, $E_e\varepsilon_0$ and $\varepsilon_0 C t^n$ refer to equilibrium and transient stress levels, respectively. Constants C, E_e and n can be determined based on the experimental relaxation results. In addition, h_e and h_2 reflect the nonlinearity in elastic properties and the rate of relaxation, respectively, which are both functions of strain (Provenzano et al., 2002). Moreover, it is hypothesized that both the linear and nonlinear parameters are correlated to the BMD.

2.5.2. Modified Superposition method (MSM)

Findley took another approach by suggesting a single power law in the form of (Findley, 1976):

$$\sigma(\varepsilon_0, t) = \varepsilon_0 Z(\varepsilon_0) t^{M(\varepsilon_0)} \tag{3}$$

where $Z(\varepsilon_0)$ and $M(\varepsilon_0)$ are functions of strain and could be obtained from isochronal stress-strain data, and from stress relaxation rate-strain data, respectively. It is assumed that both Z and M are also functions of the BMD, representing the initial stress relaxation modulus and the rate of relaxation respectively. Different than in the SSM formulation, the exponent (M) in the MSM is not a constant value and is dependent on the strain.

3. Results

The first part of this section focuses on presenting the results from the 24-h experiment, which aimed to examine the stress relaxation duration in bovine trabecular bone while also optimizing fit accuracy and experimental testing time. Subsequently, two nonlinear viscoelastic models were used to capture the stress relaxation of trabecular bone, utilizing the experimental data obtained from the repeated stress relaxation experiments. Both a sample-by-sample approach and a group-based approach were employed, and the model fits were compared to each other. Furthermore, the influence of BMD on the stress relaxation is shown.

3.1. Duration of stress relaxation

In total 16 samples were subjected to 24 h of constant strain, varying from 0.14 to 0.75 % actual strain measured optically, whereas the target was 0.2–0.8 % strain. The range of BMD of the bone samples was 229.3–562.3 mg/cm^3. All samples showed a typical stress relaxation response, which can be seen in Fig. 4 using the load, normalized to full scale. After 24 h, stress relaxation ranging from 41.0 to 68.7 % was observed. Both applied strain level and BMD did not show any significant effect on the level of stress relaxation. Large proportions of stress relaxation occurred in the first 10 min in which the maximal peak force (the maximally measured load directly after the strain is applied) decreased by 25.6–52.9 % (Fig. 5).

3.1.1. Experimental testing time

The experimental data of the 16 samples from the 24-h stress relaxation experiments were used to optimize the fit accuracy and experimental testing time. First, the stress relaxation modulus was calculated using the actual strain, measured using the camera system and the experimental load. 10 Minutes to 2 h of experimental data were extrapolated with a first order power law (extrapolated fit or EF) and compared to a power law fit of the original 24-h data (original fit or OF). These calculations were conducted for each sample, and the results for one sample are displayed in Fig. 6.

The mean accumulated percentual error was then compared between the different extrapolated fits and the original fit. The extrapolated fit from 10 min experimental data showed the highest percentual error of 18.5 % and 2 h the lowest mean error of 5.4 % (Fig. 7).

A holding time of 30 min showed an acceptable compromise between fit accuracy and experimental testing time. Therefore, the subsequent repeated stress relaxation experiments were executed with a constant displacement for 30 min.

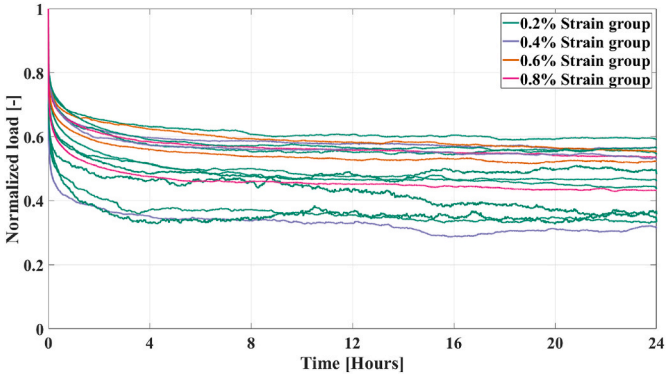

Fig. 4. Experimental stress relaxation for 24 h of constant strain for all applied strain levels. The optically measured strain level was used to assign the samples to the different strain groups.

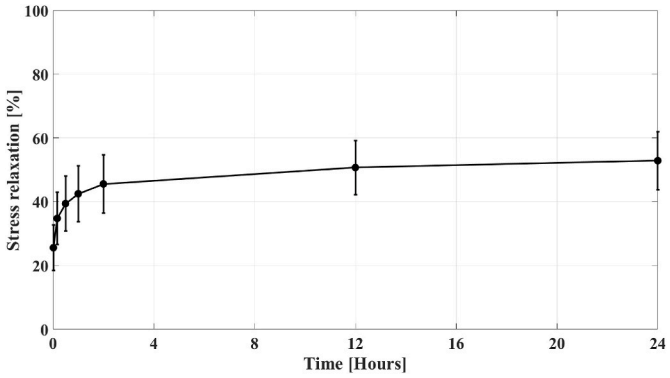

Fig. 5. The average amount of of stress relaxation and its standard deviation of various experimental time points, without strain level taken into account.

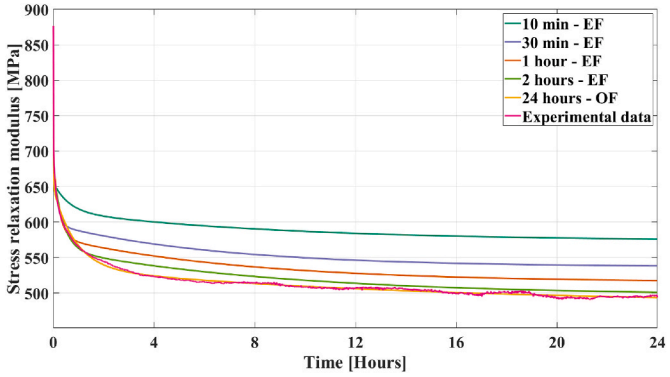

Fig. 6. Typical behavior when comparing extrapolated fits and the 24-h experimental data/fit. The sample displayed here underwent 0.49 % strain and has a BMD of 335.1 mg/cm^3.

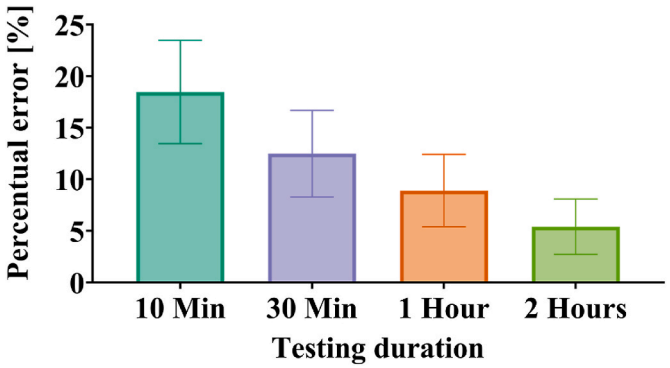

Fig. 7. Mean accumulated percentual errors and standard deviation when comparing the fits on the experimental data of different durations extrapolated to 24 h to the original 24-h fit on the experimental data.

3.2. Repeated stress relaxation

Although the intention was to impose strains ranging from 0.2 to 0.8 %, in reality, the strains, optically measured, were for the 4 levels: 0.19 ± 0.02 %; 0.34 ± 0.05 %; 0.49 ± 0.06 %; and 0.62 ± 0.09 %. The BMD range of the samples was 210.4–503.9 mg/cm^3. The experimental data were extrapolated using a first order power law to 24 h.

3.2.1. Influence of BMD on viscoelasticity

To quantify the influence of the bone mineral density on the viscoelastic properties, first it was verified if the bone mineral density actually influenced the time-dependent properties. For the different strain levels, the spearman correlation between bone mineral density and the stress relaxation rates (the slope of the log-log stress relaxation (stress vs. time)) was calculated. A very weak negative correlation (−0.322; p = 0.007) was found between bone density and the stress relaxation rate, which is the slope of the log-log time-stress curve (Fig. 8).

3.3. Quantification of nonlinear viscoelastic parameters

3.3.1. Sample-by-sample model fit

The Schapery method and the Modified Superposition method were used to determine the nonlinear viscoelastic parameters for each sample individually. This is shown for a single sample in Fig. 9. The linear and nonlinear viscoelastic model parameters for all the samples are presented for both models in Appendix A and Appendix B.

To determine the accuracy of both models to the experimental data, the initial stress relaxation modulus (the initial modulus calculated using the maximal stress and the actual applied strain), and the stress relaxation rate (the slope of the log-log time-stress curve), were compared for the different models at each strain level (Fig. 10).

Both the MSM and the SSM models show a good resemblance with the experimental results for the initial modulus and the relaxation rate. The initial stress relaxation modulus demonstrated a high variety between samples, while this was limited for the stress relaxation rate.

3.3.2. Group-based model fit

In the previous approach a sample-by-sample approach was used to fit the two models. To obtain a more global overview of the viscoelastic behavior and the effect of bone density and strain level, a group-based model fit, using the BMD values and the actual applied strain levels of all samples simultaneously, was performed. However, given the weak correlation between the BMD and the stress relaxation rate (3.2.1), it was assumed that the BMD and the stress relaxation rate were not correlated, meaning that the BMD did not influence the time-dependent properties. As earlier mentioned, the effect of BMD on the time-independent properties is already established (Morgan et al., 2003; Keyak et al., 2005). Since the time-dependent and the time-independent properties cannot be separated in the SSM model, only the MSM model was used in these further analyses.

In the MSM (equation (3)), the M parameter accounts for the time-independent properties and was correlated to both BMD and the initial strain, while the Z parameter, accounting for the time-dependent properties, was assumed to only be dependent on the strain level, resulting in equation (4). The numerical values of the nonlinear viscoelastic parameters are presented in Table 1.

$$\sigma(\varphi,\varepsilon,t) = \left(A\varepsilon + \left(B^{*}\varphi^{C} + D\right)\right)^{*}\varepsilon t^{E\varepsilon^{F}+G} \tag{4}$$

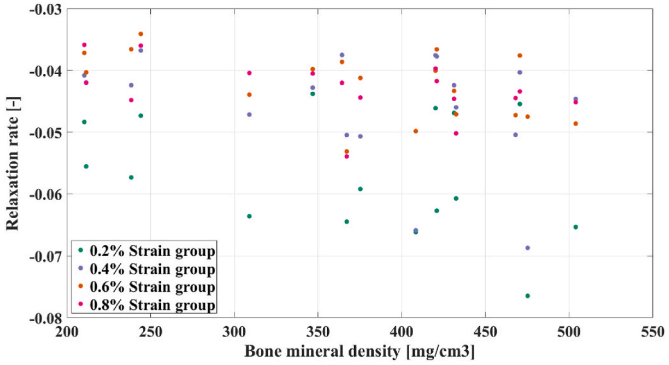

Fig. 8. The BMD versus the stress relaxation rate for all the 18 samples per strain level. The optically measured strain level was used to assign the samples to the different strain groups.

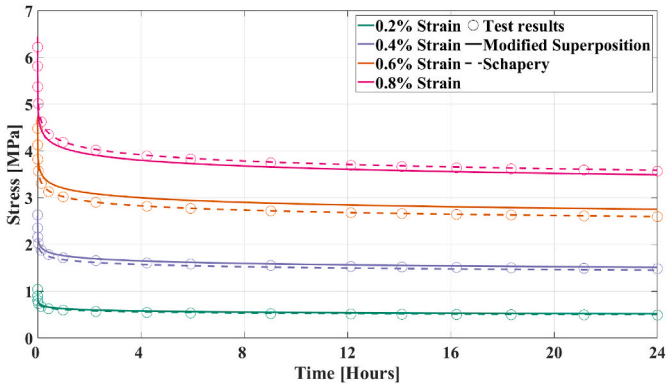

Fig. 9. An example of sample-based fitting on the experimental results of the repeated stress relaxation experiments of a sample with a BMD of 432.4 mg/cm^3 using the Modified Superposition (MSM) and Simplified Schapery (SSM) models.

The material model based on the group-based model fit led to a reduced accuracy of the prediction of the experimental results, in comparison to the method used in of 3.3.1.

In Fig. 11, an example of an accurate fit and a poor fit using the group-based MSM model can be observed. For both samples, it is shown that the actual shape of the MSM and the experimental results for the corresponding strain did match, while the absolute values of stress did not. As previously explained, the A-term of the MSM relates to the initial modulus and therefore corresponds to the absolute values (and the starting point of the stress relaxation curve). Moreover, a large difference in fit accuracy can be observed between the two samples depicted in Fig. 11.

The initial moduli and stress relaxation rates are displayed per strain level in Fig. 12. The highlighted icons resemble the samples in Fig. 11.

4. Discussion

The aim of this study was threefold: 1) To investigate the duration of stress relaxation in bovine trabecular bone; 2) to construct a material model that describes the nonlinear viscoelastic behavior of uniaxial stress relaxation experiments on bovine trabecular bone; and 3) to implement bone density into this model.

In line with these objectives, it was demonstrated that the majority of stress relaxation of the trabecular bone occurs during the first 10 min, but it did not level off completely after 24 h of constant strain. Moreover, a material model for the nonlinear stress relaxation of bovine trabecular bone was developed using two different models. Both nonlinear material models showed accurate predictions of the nonlinear viscoelastic behavior when examining a single sample. However, this accuracy was significantly decreased when a group-based model was constructed using the Modified Superposition model. The time-dependent behavior did not show a correlation with BMD, but, as expected, was found to be

Table 1
Parameters for the stress function $\sigma(\varphi, \varepsilon, t)$ displayed in equation (4).

Nonlinear viscoelastic parameters		
$A = 4.34 \times 10^4$	$D = 670$	$G = -3.86 \times 10^2$
$B = -5.14 \times 10^{10}$	$E = -3.63 \times 10^{-6}$	
$C = -3.61$	$F = -1.35$	

nonlinearly influenced by the applied strain (Quaglini et al., 2009; Yamamoto et al., 2006; Bowman et al., 1998).

In contrast with other studies, we found that even after 24 h of constant strain the stress relaxation did not level off completely: After 10 min an average stress relaxation of 35 % was observed, which increased to 53 % after 24 h (Quaglini et al., 2009; Manda et al., 2016, 2017). However, in the previously mentioned studies typically a holding time of up to 10 min (600 s) was used, which means on average 18 % of the total stress relaxation that would occur in 24 h was missed. However, an experimental time of 24 h may not be feasible when examining large numbers of specimens. Our study demonstrated that extrapolating data from a testing period of 30 min to 24 h provides a good compromise between accuracy and testing time, but when a higher accuracy is desired, longer testing is advisable. However, increasing the testing period from 30 min to 1 h only results in a slight decrease in the percentual error, from 12.5 % to 8.9 %.

While the testing time in our study was different from other studies, the stress relaxation could be compared during the first 100 s of testing. Deligianni et al. found on average 20 % stress relaxation in comparison to the observed 27 % after 100 s in the current study (Deligianni et al., 1994). Quaglini et al. observed only 10 % of stress relaxation in same time period (Quaglini et al., 2009). However, they defatted the specimens from the bone marrow, which is known to have a significant effect on the viscoelastic behavior (Linde, 1994).

Our experiments showed that as the strain increased, the rate of stress relaxation decreased in a non-linear fashion, indicating less stress relaxation is occurring. This finding is consistent with previous research (Quaglini et al., 2009). However, the exact reason for this behavior is unknown. Possibly, marrow is pushed out of the samples at higher strain values, which may affect the viscoelastic response (Linde, 1994). Alternatively, it can be hypothesized that due to higher compression the pore size decreases, which limits the outflow of water and decreases the viscoelastic behavior.

For the second objective, a simplified Schapery model and a Modified Superposition model were used for a specimen-specific fit (which excluded the influence of BMD on the viscoelastic behavior) of the uniaxial stress relaxation experiments. These models have previously been succesfully used to describe stress relaxation of other tissues, such as ligaments and dentin (Emamian et al., 2021; Provenzano et al., 2002). In this study, both models captured the nonlinear stress relaxation of trabecular bone with great accuracy.

Most studies into the viscoelastic properties of trabecular bone and other biological tissues exclusively use the aforementioned specimen-specific approach, which hinders the prediction of the time-dependent

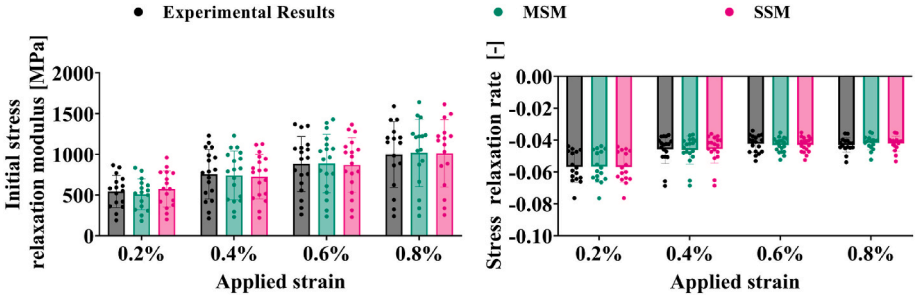

Fig. 10. On the left side, the initial stress relaxation modulus is displayed for the experimental results, the MSM and the SSM models. On the right side, the stress relaxation rate is shown for the experimental results, the MSM and the SSM models. MSM and SSM models were calculated based on four strain levels per sample.

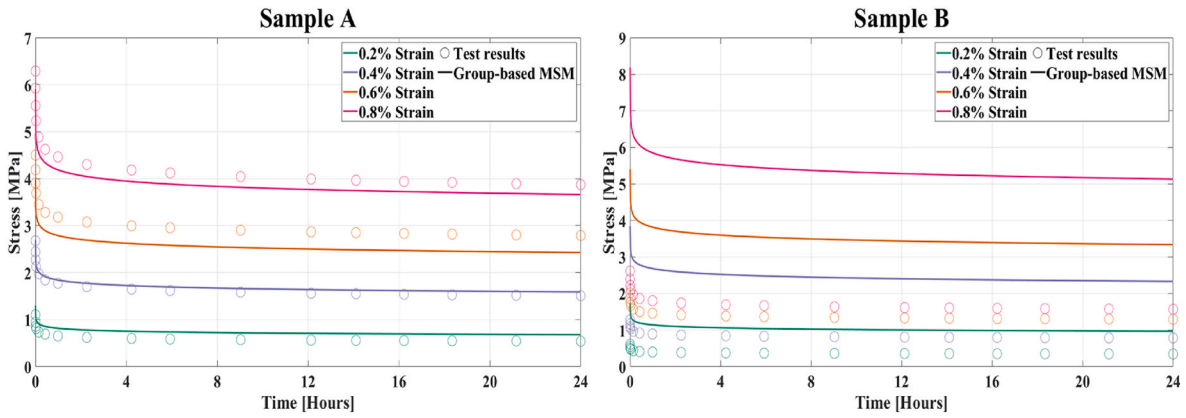

Fig. 11. Time versus stress for the four strain levels for two samples with a density of: A) 375.3 mg/cm3; B) 470.5 mg/cm3 using the group-based MSM model.

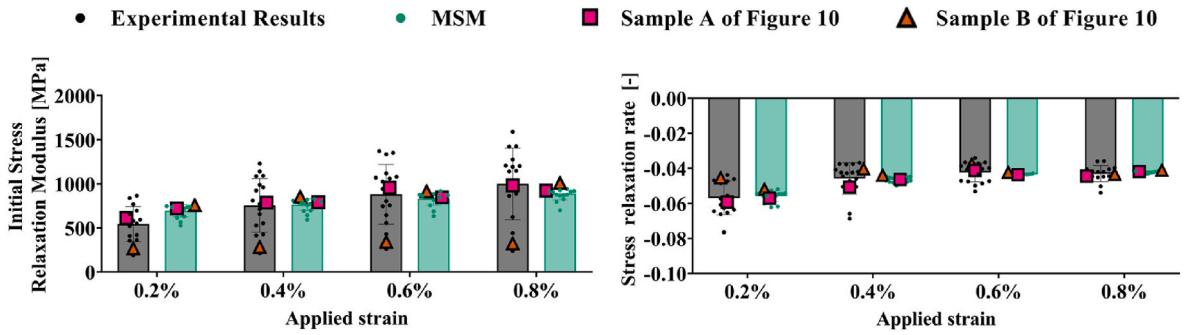

Fig. 12. Left: The initial stress relaxation modulus is displayed for the experimental results and the BMD-dependent MSM per strain level. Right: Stress relaxation rate is shown for the experimental results and calculated from the BMD-dependent MSM material model per strain level. The highlighted samples show the samples which are displayed in Fig. 11.

response in a population (Quaglini et al., 2009; Manda et al., 2017; Emamian et al., 2021; Provenzano et al., 2002). This study also implemented a group-based fitting approach, incorporating both the applied strain and the BMD as input factors. However, when all samples were considered and BMD was taken into account, the accuracy of the models decreased significantly.

Surprisingly, BMD did not influence the time-dependent behavior, which contrasts with the findings of Manda et al., 2016, 2017. However, these results support the idea that bone viscoelasticity is solely influenced by collagen (Bowman et al., 1999). In this study, the collagen content of the bone specimens was not determined to verify comparable levels of collagen among the samples, despite variations in BMD.

Since the BMD exclusively influenced the time-independent mechanical behavior investigated in this study, rather than the stress relaxation, it is crucial to distinguish between the elastic and viscoelastic properties in the material models. However, the SSM model is unable to separate elastic and viscoelastic properties and thereby was not suitable for fitting the group-based model. The MSM model is separable and therefore, the experimental results were fitted with an adapted version of this model (Equation (4)). The MSM model demonstrated a high variation in the accuracy of predicted stress relaxation between different samples (Fig. 11). The model showed less variability in the initial stress relaxation modulus (term Z in Equation (3)) than what was found in the experimental results for all strain levels. Therefore, the MSM model is capable of predicting the stress relaxation behavior of bone with an average initial modulus at each strain level, while for samples with an initial modulus which deviates greatly from the average modulus, the accuracy of the predictive capabilities of the MSM decreases vastly. The large variability in initial stress relaxation modulus observed in the experiments could be caused by the method to calculate this modulus. In this study, the measured stiffness or initial stress relaxation modulus was determined by calculating the initial apparent modulus (at t = 0.001s) for each strain, which is the tangent of two data points. However, traditionally the apparent modulus is calculated over a larger range of strain levels (e.g., 0.2 %–0.7 % strain), which provides a higher accuracy of the tangent modulus.

In this study bovine tissue was used as an alternative material for human trabecular bone. Considering that the strength and stiffness of bovine trabecular bone are comparable to that of human trabecular bone, it can be hypothesized that their viscoelastic properties are also similar (Oftadeh et al., 2015; Poumarat et al., 1993). Consequently, this study holds the potential to be employed in simulations of various orthopedic applications, providing a reliable first estimate of the viscoelastic response. In the event that varying levels of stress relaxation are observed between bovine and human trabecular bone in the future, the multiple stress relaxation protocol developed in this work establishes a solid foundation for experiments at investigating the time-dependent behavior of human trabecular bone. Due to the limited sample size the anatomical location of the samples was not taken into account. As the anatomical location does have an effect on the stiffness of the trabecular bone, future research should include its effect on the viscoelastic behavior (Morgan et al., 2003).

Despite the limitations, the newly developed material model is useful for implementing in simulations of many orthopedic applications, since samples close to the average relaxation modulus of the experimental results could be predicted accurately, which is displayed in Fig. 11A and 12. The sample of Fig. 11B showed an experimentally measured initial modulus on the lower end, which led to a significant difference in the calculated modulus using the MSM, which can be seen in Fig. 12. Furthermore, the experimentally measured stress relaxation does correspond with the determined stress relaxation rate by the MSM.

This study provides valuable insights into the stress relaxation of

trabecular bone under constant loading for up to 24 h. While longer testing may not always be practical, we recommend holding the constant strain for a minimum of 30 min and extrapolating the data to 24 h. When incorporating the time-dependent response of bone in finite element models, it is important to simulate this 24-h period, considering the large amount of stress relaxation that still occurs on the longer term. The significant level of stress relaxation observed in trabecular bone highlights the importance of incorporating viscoelastic behavior in orthopedic simulations, such as those related to implant fixation, to ensure more accurate results.

Funding

This collaboration project is co-funded by the PPP allowance made available by Health~Holland, Top Sector Life Sciences & Health, to stimulate public-private partnerships, and DePuy Synthes (Leeds, UK).

CRediT authorship contribution statement

Thomas Gersie: Writing – original draft, Visualization, Validation, Software, Project administration, Methodology, Investigation, Formal analysis, Data curation, Conceptualization. **Thom Bitter:** Writing – review & editing, Validation, Supervision, Resources, Project administration, Methodology, Conceptualization. **David Wolfson:** Writing – review & editing, Validation, Supervision, Methodology, Conceptualization. **Robert Freeman:** Writing – review & editing, Validation, Supervision, Methodology, Conceptualization. **Nico Verdonschot:** Writing – review & editing, Validation, Supervision, Resources, Project administration, Methodology, Conceptualization. **Dennis Janssen:** Writing – review & editing, Validation, Supervision, Resources, Project administration, Methodology, Funding acquisition, Conceptualization.

Declaration of competing interest

Two authors are employees of Depuy Synthes, however due to the fundamental nature of this study, there are no competing financial interests or personal relationships that could have appeared to influence the work in this paper.

Data availability

Data will be made available on request.

Acknowledgements

We would like to thank Richard van Swam for the support during the experimental tests and Max Bakker for the Matlab support.

Appendix A

Linear and nonlinear viscoelastic parameters at multiple strain levels for all 18 samples derived from the Simplified Schapery model.

BMD [mg/cm3]	Actual strain [%]	Parameters of the linear model from ε1		Parameters of nonlinear models			
		Ee [Mpa]		he [-]		h2 [-]	
		Ee = C*tˆn		y = A*εˆB + C		y = A*εˆB + C	
210.4	0.15	**C**	708.7	**A**	7.07	**A**	8.52
	0.30	**n**	−0.05	**B**	0.23	**B**	0.42
	0.40	**Ee**	409.0	**C**	−1.57	**C**	0.45
	0.55						
211.5	0.23	**C**	184.1	**A**	−1.61E-11	**A**	−0.03
	0.41	**n**	−0.06	**B**	−3.95	**B**	−0.36
	0.51	**Ee**	97.9	**C**	0.43	**C**	1.28
	0.76						
238.4	0.18	**C**	425.0	**A**	−3.44E-11	**A**	9.52E-17
	0.37	**n**	−0.06	**B**	−3.66	**B**	−5.56
	0.58	**Ee**	221.5	**C**	0.38	**C**	0.83
	0.76						
244.2	0.19	**C**	831.4	**A**	−2.83E-07	**A**	−0.18
	0.33	**n**	−0.05	**B**	−2.32	**B**	−0.32
	0.48	**Ee**	485.3	**C**	0.58	**C**	2.39
	0.64						
309.0	0.20	**C**	326.9	**A**	140.60	**A**	1.04 E+04
	0.41	**n**	−0.06	**B**	0.91	**B**	1.96
	0.53	**Ee**	158.7	**C**	−0.48	**C**	0.92
	0.69						
346.8	0.20	**C**	555.9	**A**	4.01	**A**	−1.79E-11
	0.29	**n**	−0.04	**B**	0.36	**B**	−3.95
	0.48	**Ee**	337.9	**C**	−0.43	**C**	1.80
	0.56						
364.3	0.15	**C**	1082.4	**A**	−3.34 E+10	**A**	−10.37
	0.30	**n**	−0.04	**B**	4.95	**B**	−0.06
	0.41	**Ee**	706.7	**C**	0.01	**C**	15.37
	0.53						
367.1	0.16	**C**	521.4	**A**	−1.83E-16	**A**	36.84
	0.32	**n**	−0.06	**B**	−5.47	**B**	0.75
	0.48	**Ee**	250.5	**C**	0.35	**C**	0.71
	0.62						
375.3	0.18	**C**	588.3	**A**	−1.18E-01	**A**	13.17
	0.34	**n**	−0.06	**B**	−0.41	**B**	0.03
	0.47	**Ee**	300.2	**C**	1.55	**C**	−9.70

(*continued on next page*)

(*continued*)

BMD [mg/cm3]	Actual strain [%]	Parameters of the linear model from ε1		Parameters of nonlinear models			
		Ee [Mpa]		he [-]		h2 [-]	
		Ee = C*tˆn		y = A*εˆB + C		y = A*εˆB + C	
	0.64						
408.3957	0.22	**C**	363.0	**A**	3.71 E+14	**A**	320.77
	0.32	**n**	−0.07	**B**	6.42	**B**	1.15
	0.49	**Ee**	171.2	**C**	−0.02	**C**	0.72
	0.61						
420.2	0.19	**C**	804.2	**A**	−1.28E-16	**A**	5.40 E+03
	0.36	**n**	−0.05	**B**	−5.62	**B**	1.87
	0.53	**Ee**	476.1	**C**	0.25	**C**	0.95
	0.67						
420.9	0.19	**C**	554.25	**A**	−2.68E-06	**A**	2.15 E+07
	0.34	**n**	−0.06	**B**	−2.07	**B**	3.33
	0.45	**Ee**	271.8	**C**	1.15	**C**	0.95
	0.58						
431.2	0.20	**C**	611.2	**A**	−8.27E-17	**A**	−1.45E-06
	0.30	**n**	−0.05	**B**	−5.66	**B**	−2.16
	0.50	**Ee**	358.6	**C**	0.16	**C**	2.00
	0.60						
432.4	0.20	**C**	487.9	**A**	−6.61E-15	**A**	2.39 E+09
	0.40	**n**	−0.06	**B**	−5.11	**B**	4.44
	0.60	**Ee**	244.7	**C**	0.42	**C**	1.02
	0.70						
468.0	0.04	**C**	789.9	**A**	1.56 E+03	**A**	−1.02E-05
	0.38	**n**	−0.05	**B**	1.64	**B**	−2.00
	0.50	**Ee**	445.2	**C**	−0.17	**C**	1.70
	0.62						
470.5	0.23	**C**	252.1	**A**	−1.07E-16	**A**	177.54
	0.45	**n**	−0.05	**B**	−5.75	**B**	1.32
	0.59	**Ee**	150.4	**C**	0.16	**C**	0.93
	0.81						
475.2	0.20	**C**	307.7	**A**	8.26 E+07	**A**	−1.74E-03
	0.29	**n**	−0.08	**B**	3.34	**B**	−1.09
	0.48	**Ee**	129.0	**C**	−0.08	**C**	2.49
	0.54						
503.9	0.15	**C**	645.1	**A**	−2.32E-05	**A**	107.69
	0.26	**n**	−0.07	**B**	−1.66	**B**	0.77
	0.40	**Ee**	307.0	**C**	1.11	**C**	0.28
	0.50						

Appendix B

Linear and nonlinear viscoelastic parameters describing the stress relaxation modulus ($Z(\varepsilon_0)$ in equation (3)) and the stress relaxation rate (($M(\varepsilon_0)$ in equation (3)) at multiple strain levels for all 18 samples derived from the Modified Superposition model.

BMD [mg/cm3]	Actual strain [%]	Parameters for linear model of Initial Relaxation Modulus [-]		Parameters for nonlinear model of Stress Relaxation Rate [-]	
		y = A*ε+B		y = A*εˆB + C	
210.4	0.15	**A**	1.11 E+05	**A**	−6.77E-04
	0.30	**B**	611.2	**B**	−0.55
	0.40			**C**	−0.02
	0.55				
211.5	0.23	**A**	1.02 E+04	**A**	−6.39E-13
	0.41	**B**	176.5	**B**	−3.93
	0.51			**C**	−0.04
	0.76				
238.4	0.18	**A**	3.41 E+03	**A**	−5.51E-13
	0.37	**B**	412.7	**B**	−3.82
	0.58			**C**	−0.04
	0.76				
244.2	0.19	**A**	1.19 E+05	**A**	−3.55E-12
	0.33	**B**	733.0	**B**	−3.51
	0.48			**C**	−0.03
	0.64				

(*continued on next page*)

(*continued*)

BMD [mg/cm3]	Actual strain [%]	Parameters for linear model of Initial Relaxation Modulus [-]		Parameters for nonlinear model of Stress Relaxation Rate [-]	
		y = A*ε+B		y = A*ε^B + C	
309.0	0.20	**A**	5.79 E+04	**A**	−1.64E-04
	0.41	**B**	222.2	**B**	−0.86
	0.53			**C**	−0.03
	0.69				
346.8	0.20	**A**	1.18 E+05	**A**	0.23
	0.29	**B**	458.9	**B**	0.65
	0.48			**C**	−0.05
	0.56				
364.3	0.15	**A**	1.47 E+05	**A**	−0.44
	0.30	**B**	676.5	**B**	0.65
	0.41			**C**	−0.03
	0.53				
367.1	0.16	**A**	6.73 E+04	**A**	−1.58E-15
	0.32	**B**	466.8	**B**	−4.61
	0.48			**C**	−0.05
	0.62				
375.3	0.18	**A**	8.40 E+04	**A**	−1.89E-05
	0.34	**B**	493.1	**B**	−1.12
	0.47			**C**	−0.04
	0.64				
408.4	0.22	**A**	8.35 E+04	**A**	4.62 E+12
	0.32	**B**	248.7	**B**	6.25
	0.49			**C**	−0.07
	0.61				
420.2	0.19	**A**	7.32 E+04	**A**	−1.63E-11
	0.36	**B**	706.2	**B**	−3.18
	0.53			**C**	−0.04
	0.67				
420.9	0.19	**A**	1.52 E+05	**A**	−1.54E-17
	0.34	**B**	288.6	**B**	−5.58
	0.45			**C**	−0.04
	0.58				
431.2	0.20	**A**	1.21 E+05	**A**	0.09
	0.30	**B**	538.8	**B**	0.65
	0.50			**C**	−0.05
	0.60				
432.4	0.20	**A**	6.83 E+04	**A**	−1.57E-17
	0.40	**B**	378.4	**B**	−5.53
	0.60			**C**	−0.05
	0.70				
468.0	0.04	**A**	1.61 E+05	**A**	0.58
	0.38	**B**	221.1	**B**	0.65
	0.50			**C**	−0.07
	0.62				
470.5	0.23	**A**	1.14 E+04	**A**	0.00
	0.45	**B**	243.9	**B**	−4.82
	0.59			**C**	−0.04
	0.81				
475.2	0.20	**A**	1.41 E+05	**A**	1.46 E+02
	0.29	**B**	89.8	**B**	1.54
	0.48			**C**	−0.09
	0.54				
503.9	0.15	**A**	2.41 E+05	**A**	−7.56E-17
	0.26	**B**	403.9	**B**	−5.11
	0.40			**C**	−0.05
	0.50				

References

Bowman, S.M., et al., 1994. Compressive creep behavior of bovine trabecular bone. J. Biomech. 27 (3), 301–310. https://doi.org/10.1016/0021-9290(94)90006-x.

Bowman, S.M., et al., 1998. Creep contributes to the fatigue behavior of bovine trabecular bone. J. Biomech. Eng. 120 (5), 647–654. https://doi.org/10.1115/1.2834757.

Bowman, S.M., et al., 1999. Results from demineralized bone creep tests suggest that collagen is responsible for the creep behavior of bone. J. Biomech. Eng. 121 (2), 253–258. https://doi.org/10.1115/1.2835112.

Bredbenner, T.L., Davy, D.T., 2006. The effect of damage on the viscoelastic behavior of human vertebral trabecular bone. J. Biomech. Eng. 128 (4), 473–480. https://doi.org/10.1115/1.2205370.

Burgers, T.A., et al., 2009. Post-yield relaxation behavior of bovine cancellous bone. J. Biomech. 42 (16), 2728–2733. https://doi.org/10.1016/j.jbiomech.2009.08.005.

Deligianni, D.D., Maris, A., Missirlis, Y.F., 1994. Stress relaxation behaviour of trabecular bone specimens. J. Biomech. 27 (12), 1469–1476. https://doi.org/10.1016/0021-9290(94)90196-1.

Derikx, L.C., et al., 2011. Implementation of asymmetric yielding in case-specific finite element models improves the prediction of femoral fractures. Comput. Methods Biomech. Biomed. Eng. 14 (2), 183–193. https://doi.org/10.1080/10255842.2010.542463.

Eggermont, F., et al., 2019. Calibration with or without phantom for fracture risk prediction in cancer patients with femoral bone metastases using CT-based finite element models. PLoS One 14 (7), e0220564. https://doi.org/10.1371/journal.pone.0220564.

Emamian, A., et al., 2021. Nonlinear viscoelastic properties of human dentin under uniaxial tension. Dent. Mater. 37 (2), e59–e68. https://doi.org/10.1016/j.dental.2020.10.025.

Findley, W.N., 1976. Creep and Relaxation of Nonlinear Viscoelastic Materials.

Keaveny, T.M., et al., 1997. Systematic and random errors in compression testing of trabecular bone. J. Orthop. Res. 15 (1), 101–110. https://doi.org/10.1002/jor.1100150115.

Keyak, J.H., et al., 2005. Predicting proximal femoral strength using structural engineering models. Clin. Orthop. Relat. Res. (437), 219–228. https://doi.org/10.1097/01.blo.0000164400.37905.22.

Kopperdahl, D.L., Keaveny, T.M., 1998. Yield strain behavior of trabecular bone. J. Biomech. 31 (7), 601–608. https://doi.org/10.1016/s0021-9290(98)00057-8.

Linde, F., 1994. Elastic and viscoelastic properties of trabecular bone by a compression testing approach. Dan. Med. Bull. 41 (2), 119–138.

Manda, K., et al., 2016. Linear viscoelasticity - bone volume fraction relationships of bovine trabecular bone. Biomech. Model. Mechanobiol. 15 (6), 1631–1640. https://doi.org/10.1007/s10237-016-0787-0.

Manda, K., et al., 2017. Nonlinear viscoelastic characterization of bovine trabecular bone. Biomech. Model. Mechanobiol. 16 (1), 173–189. https://doi.org/10.1007/s10237-016-0809-y.

Morgan, E.F., Bayraktar, H.H., Keaveny, T.M., 2003. Trabecular bone modulus-density relationships depend on anatomic site. J. Biomech. 36 (7), 897–904. https://doi.org/10.1016/s0021-9290(03)00071-x.

Oftadeh, R., et al., 2015. Biomechanics and mechanobiology of trabecular bone: a review. J. Biomech. Eng. 137 (1), 0108021-01080215 https://doi.org/10.1115/1.4029176.

Pankaj, P., 2013. Patient-specific modelling of bone and bone-implant systems: the challenges. Int J Numer Method Biomed Eng 29 (2), 233–249. https://doi.org/10.1002/cnm.2536.

Poumarat, G., Squire, P., 1993. Comparison of mechanical properties of human, bovine bone and a new processed bone xenograft. Biomaterials 14 (5), 337–340. https://doi.org/10.1016/0142-9612(93)90051-3.

Provenzano, P.P., et al., 2002. Application of nonlinear viscoelastic models to describe ligament behavior. Biomech. Model. Mechanobiol. 1 (1), 45–57. https://doi.org/10.1007/s10237-002-0004-1.

Quaglini, V., La Russa, V., Corneo, S., 2009. Nonlinear stress relaxation of trabecular bone. Mech. Res. Commun. 36 (3), 275–283. https://doi.org/10.1016/j.mechrescom.2008.10.012.

Schapery, R.A., 1969. On characterization of nonlinear viscoelastic materials. Polym. Eng. Sci. 9 (4), 295–+. https://doi.org/10.1002/pen.760090410.

Schoenfeld, C.M., Lautenschlager, E.P., Meyer Jr., P.R., 1974. Mechanical properties of human cancellous bone in the femoral head. Med. Biol. Eng. 12 (3), 313–317. https://doi.org/10.1007/BF02477797.

Taylor, M., Barrett, D.S., Deffenbaugh, D., 2012. Influence of loading and activity on the primary stability of cementless tibial trays. J. Orthop. Res. 30 (9), 1362–1368. https://doi.org/10.1002/jor.22056.

van der Ploeg, B., et al., 2012. Toward a more realistic prediction of peri-prosthetic micromotions. J. Orthop. Res. 30 (7), 1147–1154. https://doi.org/10.1002/jor.22041.

Yamamoto, E., et al., 2006. Development of residual strains in human vertebral trabecular bone after prolonged static and cyclic loading at low load levels. J. Biomech. 39 (10), 1812–1818. https://doi.org/10.1016/j.jbiomech.2005.05.017.

Zhao, S., et al., 2018. Standardizing compression testing for measuring the stiffness of human bone. Bone Joint Res 7 (8), 524–538. https://doi.org/10.1302/2046-3758.78.BJR-2018-0025.R1.

Zilch, H., et al., 1978. Material properties of femoral cancellous bone in axial loading. Part II: time dependent properties. Arch Orthop Trauma Surg 97 (4), 257–262. https://doi.org/10.1007/BF00380706, 1980.